Mechanism of SMYD2 promoting stemness maintenance of bladder cancer stem cells by regulating PYCR1 expression and PINK1/Parkin mitophagy pathway

JUNJIE CHEN[1], SHUAI XIAO[1], XIEYU YAN[1], YONGBAO WEI[2] and WEI SONG[1]

[1]Department of Urology, Hunan Provincial People's Hospital, The First Affiliated Hospital of Hunan Normal University, Changsha, Hunan 410011, P.R. China; [2]Shengli Clinical Medical College of Fujian Medical University, Department of Urology, Fujian Provincial Hospital, Fuzhou University Affiliated Provincial Hospital, Fuzhou, Fujian 350001, P.R. China

Received July 31, 2024; Accepted February 12, 2025

DOI: 10.3892/ijo.2025.5747

Abstract. SET and MYND domain-containing protein 2 (SMYD2), an identified protein-lysine methyltransferase, is key for bladder cancer (BC) progression. The tumor-formation capacity and metastatic potential of bladder cancer stem cells (BCSCs) are due to their stemness characteristics. The present study explores the mechanism of SMYD2 in promoting BCSC stemness maintenance by pyrroline-5-carboxylate reductase 1 (PYCR1). BC cells were treated with PYCR1, SMYD2 and putative kinase 1 (PINK1) small interfering (si)RNA, pcDNA3.1-PYCR1 and pcDNA3.1-SMYD2. Mito-Tracker Green and light chain-3B (LC3B) expression, *in vitro* colony formation ability and tumor stemness were assessed, as well as histone H3 lysine 4 trimethylation (H3K4me3) enrichment and PYCR1, SMYD2, H3K4me3, LC3B II/I, p62, PINK1, Parkin, Nanog and SRY-box transcription factor 2 (Sox2) expression. A nude mouse xenograft model was used for *in vivo* verification. PYCR1 mRNA and protein expression were elevated in BCSCs. Following PYCR1 or SMYD2 siRNA treatment, PYCR1, SMYD2 and $CD44^{+}CD33^{+}$ expression, cancer cell colony formation, number of tumor spheres and Nanog and Sox2 expression were decreased, but pcDNA3.1-PYCR1 or pcDNA3.1-SMYD2 transfection enhanced BCSC stemness maintenance. SMYD2 was associated with PYCR1 expression. SMYD2 upregulated PYCR1 expression through H3K4me3, subsequently activating the PINK1/Parkin mitophagy pathway, which supports maintenance of BCSC stemness.

Correspondence to: Dr Wei Song, Department of Urology, Hunan Provincial People's Hospital, The First Affiliated Hospital of Hunan Normal University, 61 West Jiefang Road, Changsha, Hunan 410011, P.R. China
E-mail: drsongw@126.com

Dr Yongbao Wei, Shengli Clinical Medical College of Fujian Medical University, Department of Urology, Fujian Provincial Hospital, Fuzhou University Affiliated Provincial Hospital, 134 Dong Street, Fuzhou, Fujian 350001, P.R. China
E-mail: weiyb@fjmu.edu.cn

Key words: SET and MYND domain containing protein 2, pyrroline-5-carboxylate reductase 1, histone H3 lysine 4 trimethylation, PINK1/Parkin, mitophagy, bladder cancer, stem cell stemness

Introduction

Cancer stem cells (CSCs) play a pivotal role in tumorigenesis and have been extensively investigated as a prospective target for anticancer therapy (1,2). An association exists between the presence of CSCs and tendencies towards recurrence, treatment resistance and immunological tolerance in bladder cancer (BC); nevertheless, the mechanisms by which bladder CSCs (BCSCs) sustain their stemness are not fully elucidated (3). Pyrroline-5-carboxylate reductase 1 (PYCR1) has been identified as a carcinogenic factor of BC and has been shown to promote BC proliferation, metastasis and epithelial-mesenchymal transition (EMT) (4-6). PYCR1 can promote proliferation, metastasis and EMT of BC, and its role is similar to that of tumor stemness; therefore (7), it is plausible to hypothesize the potential role of PYCR1 in the regulation of BCSC stemness.

Histone methylation, a well-known epigenetic modification mediated by histone demethylases, methyltransferases and methylation reader proteins, is instrumental in cancer pathogenesis (8). SET and MYND domain-containing protein 2 (SMYD2) is a protein methyltransferase, including a catalytic SET domain, known to facilitate monomethylation of lysine residues on both histone and non-histone proteins (8,9). Expression of SMYD2 is significantly enhanced in breast cancer tissues, and patients with BC with elevated SMYD2 expression show a poor prognosis (10). Elevated levels of SMYD2 may promote the proliferation of papillary thyroid carcinoma cells (11), as well as regulate gene expression by modulating histone H3 lysine 4 trimethylation (H3K4me3) modification in the promoter region of its target gene, thereby affecting gastric cancer cell glycolysis and proliferation (12). It was proposed that SMYD2 may stimulate the transcriptional expression of PYCR1 by regulating the levels of H3K4me3 in the promoter region of PYCR1 to regulate BC stemness.

Mitophagy facilitates maintenance of stemness in CSCs (13,14). Mitophagy enhances the plasticity of CSCs via metabolic recombination, thereby improving their adaptation to the tumor microenvironment (15). The putative kinase 1 (PINK1)/Parkin signaling pathway is one of the key mechanisms regulating mitophagy (16,17). When the PINK1/Parkin mitophagy pathway is stimulated, SRY-box transcription factor 2 (Sox2) promotes Nanog expression, potentiates CSC self-renewal and preserves CSC stemness (18). PYCR1/2 serves as a crucial enzyme in the proline biosynthetic pathway, and proline is capable of inducing mitophagy via activation of AMPKα and the upregulation of the Parkin expression (19). Our previous study revealed that overexpression of PYCR1 has the potential to boost the protein expression of PINK1 and Parkin, leading to mitophagy in BC (4). Also, PYCR1-augmented proline synthesis serves a crucial role in sustaining the stemness of CSCs (20). Therefore, PYCR1 might regulate BCSC stemness by controlling mitophagy via the PINK1/Parkin pathway. It was hypothesized that SMYD2 may increase PYCR1 expression by upregulating the H3K4me3 levels in the PYCR1 promoter region and promote BCSC stemness through PINK1/Parkin-regulated mitophagy.

Materials and methods

Bioinformatics analysis. SMYD2 expression in BC and normal bladder tissue and the association between SMYD2 and PYCR1 in BC were analyzed using the GEPIA database (gepia.cancer-pku.cn/).

Cell culture and grouping. Human BC cell lines T24 (SCSP-536) and EJ (YS1803C) were procured from Institute of Chinese Academy of Sciences and Yaji Biotechnology Co., Ltd. (both Shanghai, China), respectively. T24 and EJ cells were cultured in DMEM/Ham's F-12 with 10% fetal bovine serum (both Gibco; Thermo Fisher Scientific, Inc.) and 1% penicillin-streptomycin solution (Shanghai Zeye Biotechnology Co., Ltd.) at 37˚C with 5% CO_2. Cells from the P3 generation with 80% confluence were collected for subsequent experiments.

Human BC cell lines were grouped as follows: Blank (untreated); small interfering (si)-PYCR1 (cells were transfected with PYCR1 siRNA for 6 h and cultured for 18 h].); si-SMYD2 (BC cells were transfected with SMYD2 siRNA for 24 h); si-negative control (NC) (transfected with scramble siRNA for 24 h); overexpression (oe)-PYCR1 (pcDNA3.1-PYCR1-transfected for 24 h); oe-SMYD2 (transfected with pcDNA3.1-SMYD2 for 24 h); oe-NC (transfected with pcDNA3.1-NC for 24 h); oe-SMYD2 + si-PYCR1 (transfection of pcDNA3.1-SMYD2 while being treated with PYCR1 siRNA for 24 h); oe-SMYD2 + si-NC (treated with scramble siRNA for 24 h while being transfected with pcDNA3.1-SMYD2); oe-PYCR1 + si-PINK1 (24-h simultaneous treatment with pcDNA3.1-PYCR1 and PINK1 siRNA) and oe-PYCR1 + si-NC group (co-treatment with pcDNA3.1-PYCR1 and scramble siRNA for 24 h). si-PYCR1 forward 5'-UGCUAUCAACGCUGUGG-3' and reverse 5'-CCACAGCGUUGAUAGCA-3'; si-SMYD2: forward: 5'-CACCAGUUCUACUCCAAGUTT-3', reverse: 5'-ACUUGGAGUAGAACUGGUGTT-3'; si-NC: forward 5'-UUCUCCGAACGUGUCACGUTT-3' and reverse 5'-ACGUGACACGUUCGGAGAATT-3'.

Cell transfection was performed using Lipofectamine 2000 (Invitrogen; Thermo Fisher Scientific, Inc.) at 37˚C for 24 h with 10 nmol/l pcDNA3.1-PYCR1, pcDNA3.1-SMYD2, pcDNA3.1-NC, PYCR1 siRNA, SMYD2 siRNA, PINK1 siRNA, and scramble siRNA, with a final concentration of 3.75 μl/ml, as previously described (21).

Flow cytometry. Cells were prepared into a single-cell suspension for the screening of BCSCs. After being washed twice with PBS, cells were resuspended in PBS to adjust the cell concentration to $1x10^9$/l. Cells were cultured in the presence of antibodies labeled with CSC markers, such as CD44 (IM7) Rat mAb (Alexa Fluor® 555 Conjugate; cat. no. #95235) and CD133 (A8N6N) Mouse mAb (Alexa Fluor® 647 Conjugate; cat. no. #53276; both 1:50; both Cell Signaling Technology, Inc.) on ice without light for 30 min, followed by PBS rinsing three times. Fluorescence-activated cell sorting Aria III (BD Biosciences) was employed to sort $CD44^+CD133^+$ cells.

Reverse transcription-quantitative (RT-q)PCR. Total RNA extraction from cells was performed using TRIzol (Invitrogen; Thermo Fisher Scientific, Inc.). Total RNA underwent RT to complementary DNA using a PrimeScript RT reagent kit (Takara Biotechnology Co., Ltd.) according to the manufacturer's instructions. qPCR was performed using TB Green® Premix Ex Taq II (Takara Biotechnology Co., Ltd.) and primers (Table I) on the ABI7900 fluorescence PCR instrument. Thermocycling conditions were as follows: Initial denaturation at 95˚C for 10 min, followed by 40 cycles of denaturation at 95˚C for 10 sec, annealing at 60˚C for 20 sec and extension at 72˚C for 34 sec. β-actin was used as the internal reference, and data analysis was conducted using the $2^{-\Delta\Delta Cq}$ method (22).

Colony formation assay. BC cells were seeded in 6 cm culture dishes at a density of $1x10^3$ cells/ml and cultured at 37˚C for 14 days to colony formation. After the culture dish was washed with distilled water, cells were immobilized at room temperature with 4% paraformaldehyde (Sigma-Aldrich; Merck KGaA) for 15 min and then stained with crystal violet (Beyotime Institute of Biotechnology) for 30 min at room temperature. Images were captured and the quantification of cell colonies was performed manually. The colony was defined as a cell population large enough to be observed with the naked eye.

CSC sphere-forming assay. Serum-free DMEM/F-12 (Gibco) was supplemented with 20 ng/ml each epidermal growth factor (Invitrogen) and basic fibroblast growth factor (Gibco; all Thermo Fisher Scientific, Inc.). Then, 5 μg/ml insulin (Procell Life Science & Technology Co., Ltd.) and 100 μg/ml penicillin/streptomycin were added to a low adhesion 6-well plate. Cells were re-suspended with 1 ml medium added to the plate every 3 days. Afterward, cells were seeded at 1,000 cells/well into DMEM/F-12 (serum-free). Following 7 days of culture at 37˚C, tumor spheres were collected once the diameter reached 50-100 μm. Spheres were detached and dispersed into single cells and re-seeded to form new tumor spheres once again.

Table I. Primer sequences.

Gene	Forward, 5'→3'	Reverse, 5'→3'
PYCR1	GGCTGCCCACAAGATAATGGC	GGCTGCCCACAAGATAATGGC
SMYD2	ATCTCCTGTACCCAACGGAAG	CACCTTGGCCTTATCCTTGTCC
β-actin	TGGCACCCAGCACAATGAA	TGGCACCCAGCACAATGAA
Nanog	CCCCAGCCTTTACTCTTCCT	CCAGGTTGAATTGTTCCAGGTC
Sox2	ATCAGGAGTTGTCAAGGCAGAG	AGAGGCAAACTGGAATCAGGA

PYCR1, pyrroline-5-carboxylate reductase 1; SMYD2, SET and MYND domain-containing protein 2; Sox2, SRY-box transcription factor 2.

After 14 days at 37˚C, the culture was terminated and the number of tumor sphere (diameter >50 μm) was calculated manually under the Leica DMi8 inverted light microscope (200X magnification).

Cell mitophagy analysis. Cells were stained at 37˚C with 400 nM Mito-Tracker Green (cat. no. #C1046, Beyotime Institute of Biotechnology) for 40 min, and then blocked at 37˚C for 1 h with 1% bovine serum albumin (BSA, cat. no. #735094; Amresco, LLC) in PBS. Following 1 h incubation at 37˚C with the primary antibody light chain-3B (LC3B; cat. no. ab192890, 1:100), the secondary antibody 6478-Conjugated Goal Anti-Rabbit IgG (cat. no. ab150083, 1:200; both Abcam) was added to cells for 30-min at 37˚C and nuclei were stained with 5 μg/ml DAPI (cat. no. #C1002; Beyotime Institute of Biotechnology) at room temperature for 3 min. Finally, the immunofluorescence was visualized using a laser confocal microscope (200x).

Chromatin immunoprecipitation (ChIP) assay. Analysis was conducted utilizing a simpleChIP®Plus ultrasonic ChIP kit (cat. no. #56383, Cell Signaling Technology, Inc.). Cells at 80% confluence were fixed using 4% paraformaldehyde at room temperature for 15 min and treated with glycine at room temperature for 15 sec at a final concentration of 0.125 M (both Beyotime Institute of Biotechnology) to halt the fixation process. Cells were lysed and centrifuged at 300 x g at 4˚C for 5 min. Chromatin was resuspended in ChIP lysis buffer (50 mM HEPES-KOH pH 7.5, 140 mM NaCl, 1 mM EDTA pH 8, 1% Triton X-100, 0.1% deoxycholate, 0.1% SDS), 1% protease inhibitor) and sonicated on ice for 2 min (sonication: 3 sec on, 2 s off) to shear DNA-protein fragments to approximately 500 bp. 20 μl of cell lysate was incubated overnight at 4˚C with 5 μg of rabbit Anti-H3K4me3 antibody (#9751S, 1:50, Cell Signaling Technology) or rabbit IgG (2729S, 1:100, Cell Signaling Technology). Protein-A beads (20 μl) were then used to capture the antibody complex. The beads were washed 7 times with wash buffer (50 mM HEPES, pH 7.5; 500 mM LiCl; 1 mM EDTA; 1% NP-40 and 0.7% deoxycholate), followed by one wash with Tris-EDTA buffer (10 mM Tris pH 8.0, 1 mM EDTA). The precipitated DNA was purified using a purification column and the expression of PYCR1 was detected by RT-qPCR as aforementioned. Primers were as follows: PYCR1-forward, 5'-CCTGTCATC ATCTAAGATAC-3'; PYCR1-reverse, 5'-CCCTGTCGGTGG CCAAGATT-3'.

In vivo xenograft experiment. BALB/C nude mice (male, n=30; age, 5 weeks; weight 20-22 g) were purchased from Experimental Animal Resource Platform of the Chinese Academy of Sciences [animal license no. SYXK (Beijing) 2021-0063, Beijing, China]. Nude mice were housed in a standard animal house (25±2˚C, 50±10% relative humidity, 12/12-h light-dark cycle and *ad libitum* access to food and water).

The BC xenograft model was established by subcutaneously injecting T24 cells ($2x10^6$ cells in 100 μl PBS) into nude mice. Mice were randomly divided (six mice/group) into groups as follows: BC; BC + lentivirus (Lv)-oe-SMYD2 (T24 cells delivered with pcDNA3.1-SMYD2 Lv were subcutaneously injected); BC + Lv-oe-NC (injection of T24 cells transfected with pcDNA3.1-NC Lv plasmid); BC + Lv-oe-SMYD2 + Lv-si-PYCR1 (T24 cells transfected with pcDNA3.1-SMYD2 + si-PYCR1 Lv plasmids were hypodermically injected); BC + Lv-oe-SMYD2 + Lv-si-NC (T24 cells transfected with pcDNA3.1-SMYD2 + si-NC Lv plasmids were subcutaneously injected). After 4 weeks, mice were euthanized via intraperitoneal injection of 100 mg/kg sodium pentobarbital and tumor tissue was obtained to measure the longest longitudinal (a) and transverse diameter (b). The tumor volume was calculated and weighed using the formula $(a \times b^2)/2$ (23), followed by protein extraction, hematoxylin-eosin (HE) staining and immunohistochemistry (IHC). The humane endpoints were body weight of the mice decreased by 40% or the tumor diameter more than 3 cm). No mice reached the humane endpoints.

Western blotting. The homogenates of cells or tumor tissues were lysed using RIPA lysis solution (Beyotime Institute of Biotechnology) containing protease inhibitors (Sigma-Aldrich; Merck KGaA) and supernatants were obtained upon 20 min centrifugation at 12,000 x g at 4˚C. Protein concentration was determined using a BCA kit. The protein loading amount of each well was 10 μg. Following separation via 10% SDS-PAGE, protein bands were moved to a PVDF membrane and incubated overnight at 4˚C with the following primary antibodies: Anti-PYCR1 (cat. no. ab226340, 1:2,000), anti-SMYD2 (cat. no. ab108217, 1:2,000), anti-Nanog (cat. no. ab21624, 1:200), anti-Sox2 (cat. no. ab92494, 1:1,000), anti-H3K4me3 (cat. no. ab272143, 1:500), anti-PINK1 (cat. no. ab216144, 1:1,000, all Abcam), anti-Parkin (cat. no. PA5-13399, 1:2,000, Invitrogen; Thermo Fisher Scientific, Inc.), anti-LC3B (cat. no. ab192890, 1:2,000), anti-p62 (cat. no. ab109012,

1:10,000) and β-actin (cat. no. ab8227, 1:1,000; all Abcam). Subsequently, the membrane was washed with TBS-tween (0.1% Tween 20; cat. no. ST673; Beyotime) and incubated with horseradish peroxidase-labeled goat anti-rabbit IgG (cat. no. ab205718, 1:2,000, Abcam) for 1 h at room temperature. Protein bands were visualized using the ultrasensitive enhanced chemiluminescence kit (cat. no. P0018S, Beyotime) and the gray values were quantified using Image J 1.8 software (National Institutes of Health), with β-actin serving as the internal reference. Cell experiments were repeated three times.

HE staining. Rat tumor tissues were subjected to paraffin embedding after fixation with 4% paraformaldehyde at room temperature for 24 hand cut into 5-μm sections. The sections were stained at room temperature for 20 min with HE Stain kit (cat. no. G1120; Beijing Solarbio Science & Technology Co., Ltd.) and photographed under a light microscope (200x) (Olympus Corporation).

IHC. The tumor tissue subjected to 24-h fixation with 4% paraformaldehyde at room temperature was embedded in paraffin, serially sectioned (4 μm), dewaxed with xylene, and hydrated with gradient alcohol. Sections were treated with 3% H_2O_2 for 10 min to neutralize endogenous peroxidase activity. The samples were subjected to antigen retrieval in 0.01 mol/l sodium citrate buffer (pH=6.0, 15 min) using microwave heating at 95˚C. The sections were blocked at room temperature for 20 min using 5% BSA (cat. no. A602440-0050, Sangon Biotechnology Co., Ltd.) and incubated overnight at 4˚C with primary antibodies against H3K4me3 (cat. no. ab8580, 1:100), SMYD2 (cat. no. ab234862, 1:200), CD44 (cat no. ab316123, 1:5,000) and CD133 (cat. no. ab19898, 1:500; all Abcam). HRP labeled goat anti rabbit IgG (cat. no. ab6721, 1:1,000; Abcam) was incubated at room temperature for 20 min. After sections were rinsed with PBS, the color was developed using 3,3'-diaminobenzidine (cat. no. B-IMWRS51, AmyJet Scientific, Inc.). The staining was observed under a light microscope (200X magnification; Olympus Corporation). The percentages of positive cells were counted and averaged using Image J 1.8 (National Institutes of Health).

Statistical analysis. All data analysis was performed using SPSS 21.0 (IBM Corp.) and GraphPad Prism 9.5 (GraphPad Software, Inc.; Dotmatics). The data are presented as the mean ± SD of three independent experiments. Comparisons between two groups were performed using unpaired t-test, while multi-group comparisons were analyzed using one-way ANOVA followed by Tukey's multiple comparison test. $P<0.05$ was considered to indicate a statistically significant difference.

Results

PYCR1 promotes stemness maintenance of BCSCs. To investigate whether PYCR1 is involved in regulating BCSC stemness, BC cell lines (EJ and T24) were cultured *in vitro*. Subpopulations exhibiting SC characteristics ($CD44^+CD133^+$) were sorted from BC cells by flow cytometry and expression of PYCR1 mRNA and proteins in $CD44^+CD133^+$ and $CD44^-CD133^-$ cells was assessed via RT-qPCR and western blot. The results showed that PYCR1 mRNA and its protein expression were higher in the $CD44^+CD133^+$ BC cell subpopulation than in $CD44^-CD133^-$ cells (Fig. 1A and B). Following PYCR1 siRNA treatment, PYCR1 mRNA and protein expression in BC cells (Fig. 1C and D), $CD44^+CD133^+$ cell levels (Fig. 1E) and colony tumor sphere formation (Fig. 1F and G) and Nanog and Sox2 expression was reduced (Fig. 1H and I). Following transfection of pcDNA3.1-PYCR1, BC cells had increased expression of PYCR1 mRNA and protein (Fig. 1C and D) levels of $CD44^+CD133^+$ cells (Fig. 1E), increased formation of cancer cell colonies and tumor spheres (Fig. 1F and G) and elevated expression of Nanog and Sox2 (Fig. 1H and I). These results indicated that PYCR1 enhanced BCSC stemness maintenance.

SMYD2 promotes stemness maintenance of BCSCs. Multiple post-translational modifications of proteins serve crucial roles in tumor progression, with methylation modification being common (24). SMYD2 is a protein lysine methyltransferase involved in the advancement of BC (10). SMYD2 was found to be significantly highly expressed in BC through the analysis of the GEPIA database (Fig. 2A). When BC cells were treated with SMYD2 siRNA, SMYD2 mRNA and protein expression (Fig. 2B and C), $CD44^+CD133^+$ cell levels (Fig. 2D), colony and tumor sphere formation (Fig. 2E and F) and Sox2 and Nanog expression decreased (Fig. 2G and H). However, following transfection of pcDNA3.1-SMYD2 into BC cells, SMYD2 mRNA and protein expression (Fig. 2B and C), levels of $CD44^+CD133^+$ cells (Fig. 2D), colony and tumor sphere formation (Fig. 2E and F) and the protein expression of stemness markers Nanog and Sox2 was increased (Fig. 2G and H). Altogether, these findings illustrated that the stemness retention of BCSCs was promoted by SMYD2.

SMYD2 modulates H3K4me3 to upregulate PYRC1 expression in BC cells. SMYD2 was positively associated with PYCR1 expression in BC according to the GEPIA database analysis (Fig. 3A). Following transfection of SMYD2 siRNA in BC cells, PYCR1 mRNA and its protein expression and H3K4me3 levels decreased, while transfection of pcDNA3.1-SMYD2 into BC cells increased PYCR1 mRNA and protein expression and H3K4me3 levels (Fig. 3B and C). ChIP assay demonstrated enrichment of H3K4me3 in the PYCR1 promoter region was decreased following SMYD2 siRNA but increased following pcDNA3.1-SMYD2 transfection (Fig. 3D). Overall, SMYD2 modulated the expression of PYRC1 in BC cells by controlling the H3K4me3 levels in the PYRC1 promoter region.

SMYD2 facilitates BCSC stemness maintenance by regulating PYCR1. To explore whether SMYD2 can promote stemness maintenance of BCSCs by modulating PYCR1, BC cells were transfected with pcDNA3.1-SMYD2 and PYCR1 siRNA. Compared with oe-SMYD2 + si-NC group, cells in the oe-SMYD2 + si-PYCR1 group exhibited decreased expression of PYCR1 mRNA and protein (Fig. 4A and B), $CD44^+CD133^+$ cell levels (Fig. 4C), colony and tumor sphere formation (Fig. 4D and E) and Nanog/Sox2 expression Fig. 4F and G). These results suggested that SMYD2 contributed to BCSC stemness maintenance by modulating expression of PYCR1.

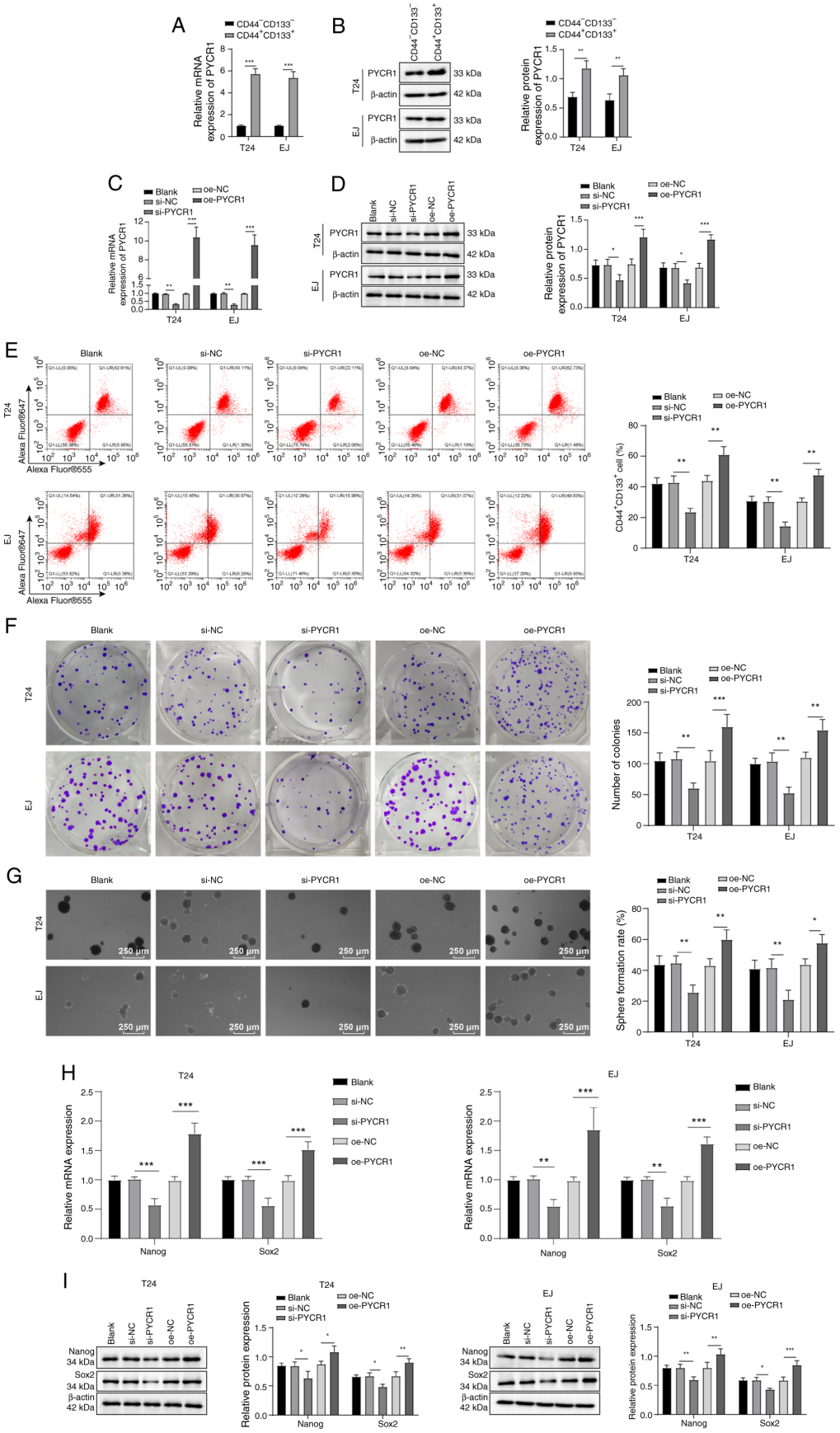

Figure 1. PYCR1 sustains bladder CSC stemness. (A) RT-qPCR and (B) western blot were used to assess PYCR1 mRNA and protein expression in $CD44^+CD133^+$ and $CD44^-CD133^-$ cells. Detection of PYCR1 (C) mRNA and (D) protein expression using western blot and RT-qPCR. (E) Detection of $CD44^+CD133^+$ cells by flow cytometry. (F) Measurement of *in vitro* colony formation ability. (G) CSC sphere-forming assay was performed to examine tumor stemness. (H) RT-qPCR and (I) western blotting were performed to assess expression of stemness marker proteins Nanog and Sox2 mRNA and protein. $^*P<0.05$, $^{**}P<0.01$, $^{***}P<0.001$. PYCR1, pyrroline-5-carboxylate reductase 1; CSC, cancer stem cell; RT-q, Reverse transcription quantitative; si, small-interfering; NC, negative control; oe, overexpression.

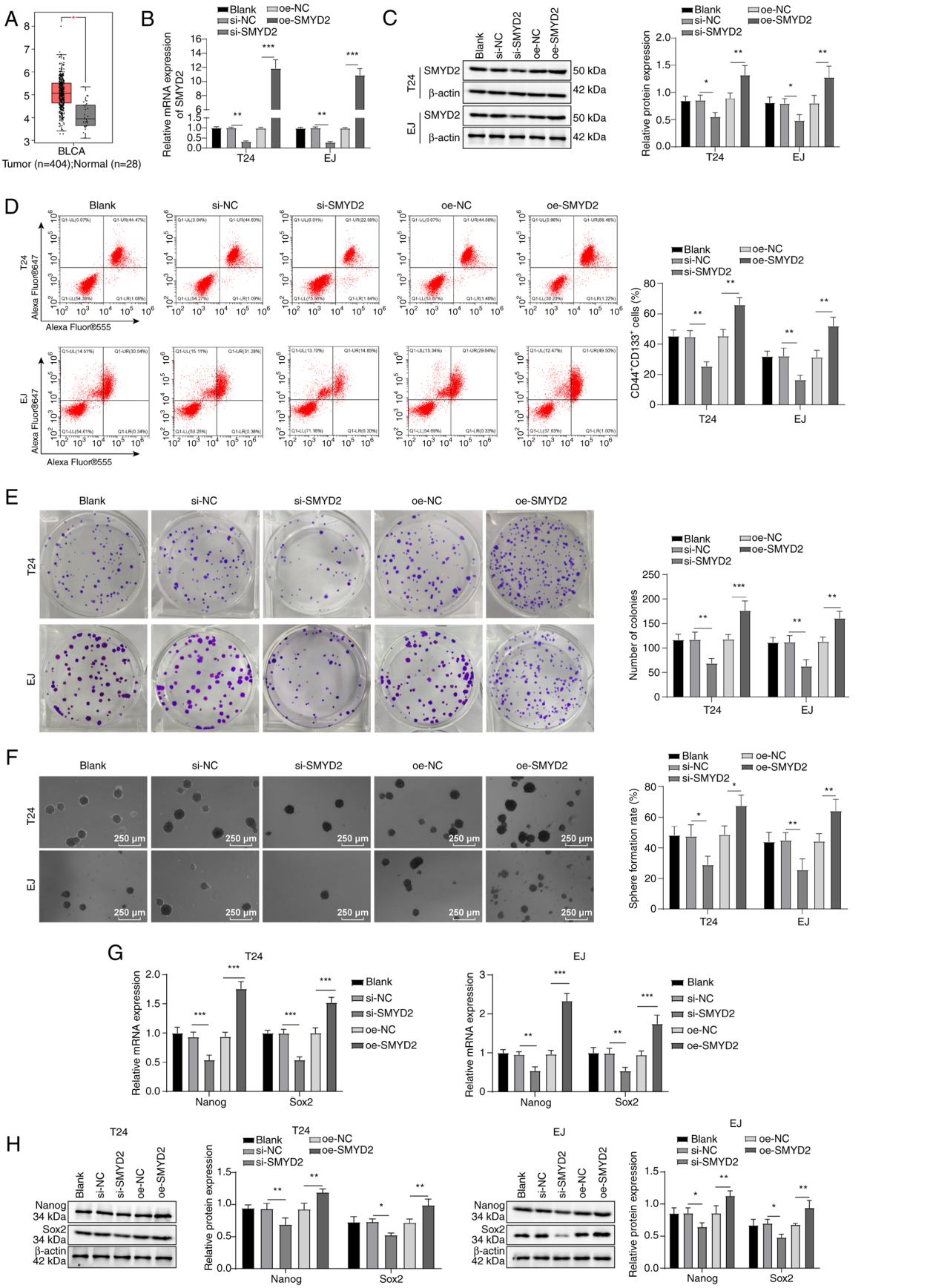

Figure 2. SMYD2 promotes stemness retention in bladder CSCs. (A) Analysis of SMYD2 expression in normal bladder tissue and bladder cancer using Gene Expression Profiling Interactive Analysis database. SMYD2 (B) mRNA and (C) protein expression using RT-qPCR and western blotting. (D) Flow cytometry to determine $CD44^+CD133^+$ cell levels. (E) *In vitro* colony formation capability. (F) CSC sphere-forming assay to examine tumor stemness. (G) RT-qPCR and (H) western blotting were used to evaluate the expression of Nanog and Sox2. $^*P<0.05$, $^{**}P<0.01$, $^{***}P<0.001$. SMYD2, SET and MYND domain-containing protein 2; CSC, cancer stem cell; RT-qPCR, reverse transcription quantitative polymerase chain reaction; si, small-interfering; NC, negative control; oe, overexpression; ns, not significant; BLCA, bladder urothelial carcinoma.

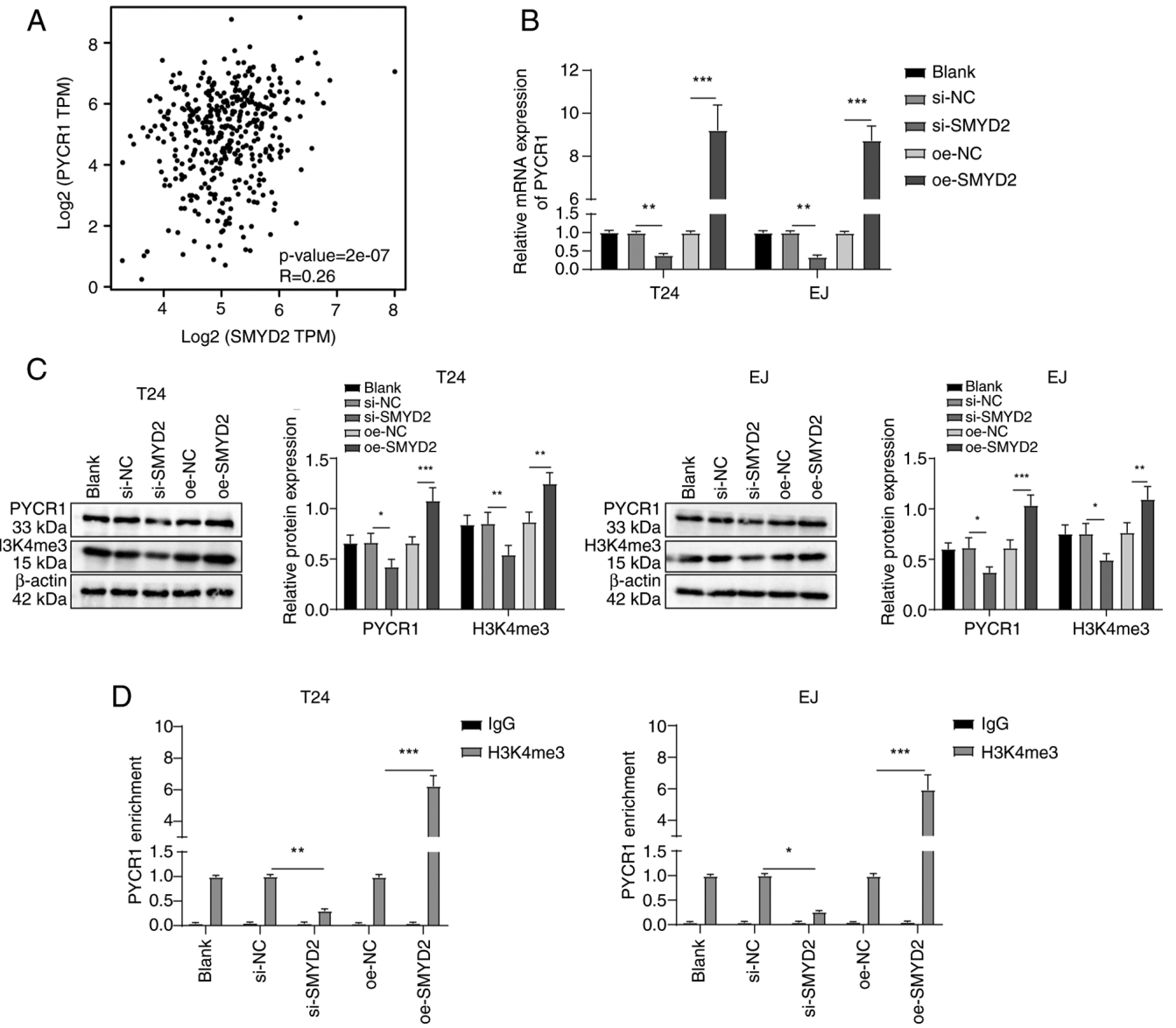

Figure 3. SMYD2 elevates PYRC1 expression via regulation of H3K4me3 methylation. (A) Gene Expression Profiling Interactive Analysis database was used to analyze SMYD2-PYCR1 correlation in BC tissue. (B) Reverse transcription-quantitative PCR was employed to evaluate expression of PYCR1 mRNA. (C) Western blotting was utilized for measuring the protein expression of PYCR1 and H3K4me3. (D) Chromatin immunoprecipitation detection of H3K4me3 enrichment in the PYCR1 promoter region. *P<0.05, **P<0.01, ***P<0.001. SMYD2, SET and MYND domain-containing protein 2; PYRC1, pyrroline-5-carboxylate reductase 1; H3K4me3, histone H3 lysine 4 trimethylation; TPM, transcripts per million; si, small-interfering; NC, negative control; oe, overexpression.

PYCR1 potentiates BCSC stemness maintenance via the PINK1/Parkin mitophagy pathway. Following PYCR1 siRNA treatment, mitochondrial LC3B expression (Fig. 5A) and LC3B II/I ratio decreased and p62 protein expression was augmented (Fig. 5B); these alterations were reversed following pcDNA3.1-PYCR1 transfection. Additionally, following treatment with PYCR1 siRNA, expression of PINK1 and Parkin proteins was decreased; after transfection of pcDNA3.1-PYCR1, expression of PINK1 and Parkin proteins increased (Fig. 5B). BC cells were transfected with PINK1 siRNA and pcDNA3.1-PYCR1. In comparison with the oe-PYCR1 + si-NC group, oe-PYCR1 + si-PINK1 group exhibited reduced PINK1/Parkin protein (Fig. 5B) and LC3B expression (Fig. 5A) and LC3B II/I ratio, raised p62 protein expression (Fig. 5B) and inhibited $CD44^{+}CD133^{+}$ cell levels (Fig. 5C), formation of tumor spheres and colonies (Fig. 5D and E) and expression of Sox2 and Nanog (Fig. 5F and G). Collectively, these findings demonstrated that PYCR1 enhanced BCSC stemness maintenance via regulation of the PINK1/Parkin mitophagy pathway.

SMYD2 strengthens BCSC stemness sustenance by activating the PINK1/Parkin mitophagy pathway via upregulation of PYCR1. A BC xenograft model was established for *in vivo* validation experiments by subcutaneously injecting T24 cells transfected with pcDNA3.1-SMYD2 or si-PYCR1 Lv plasmid into nude mice. Tumor size and weight in the BC + Lv-oe-SMYD2 group were higher than those in the BC + Lv-oe-NC group; tumor weight and size in the BC + Lv-oe-SMYD2 + Lv-si-PYCR1 group were lower than

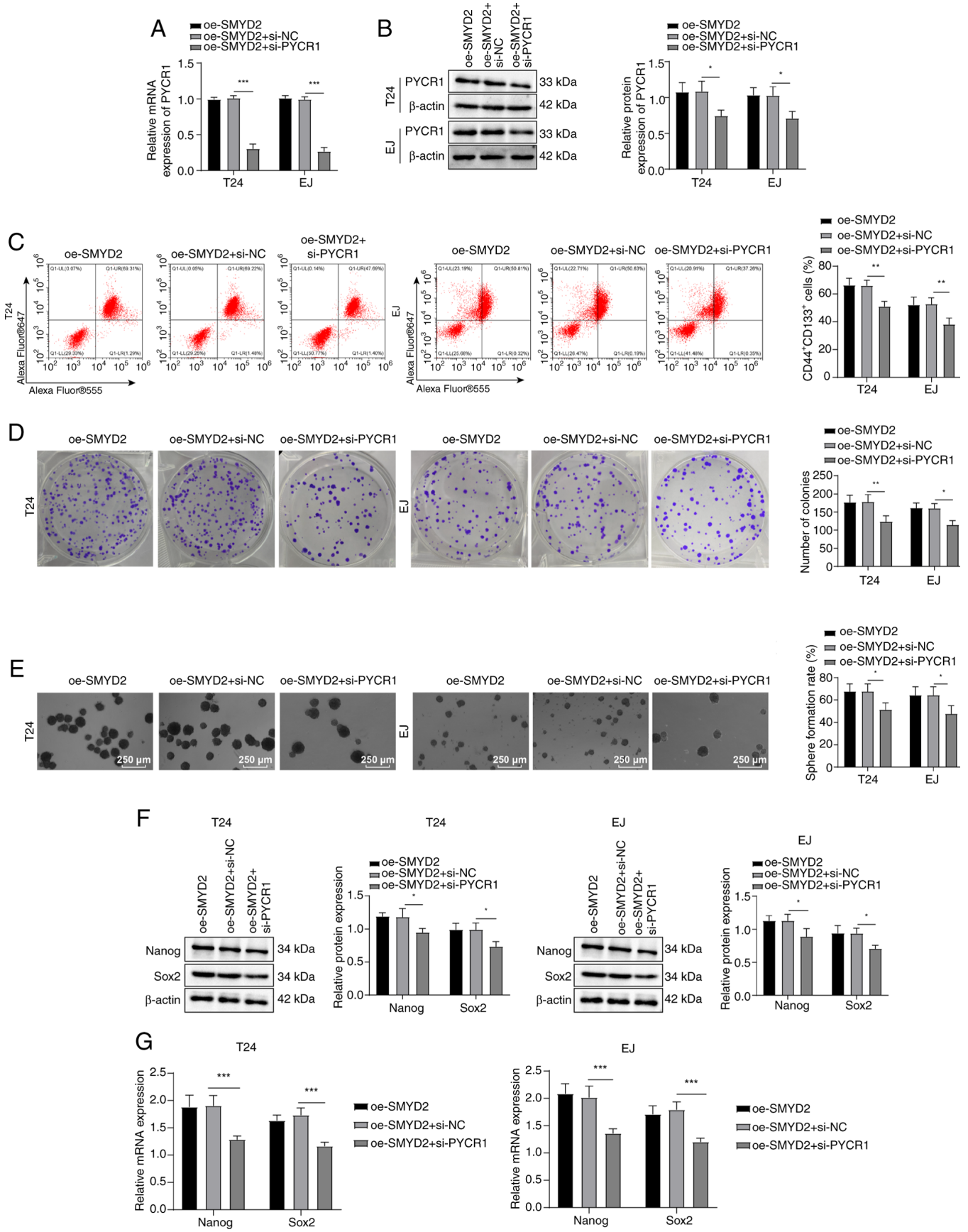

Figure 4. SMYD2 regulates PYCR1 expression to potentiate bladder SCS stemness. PYCR1 (A) mRNA and (B) protein expression by reverse transcription-quantitative PCR and western blot. (C) Assessment of $CD44^{+}CD133^{+}$ cell level by flow cytometry. (D) *In vitro* colony formation ability. (E) Tumor stemness testing utilizing CSC sphere-forming assay. Examination of Sox2 and Nanog (F) mRNA and (G) protein expression by RT-qPCR and western blot. *P<0.05, **P<0.01, ***P<0.001. SMYD2, SET and MYND domain-containing protein 2; PYRC1, pyrroline-5-carboxylate reductase 1; si, small-interfering; NC, negative control; oe, overexpression; CSC, cancer stem cell.

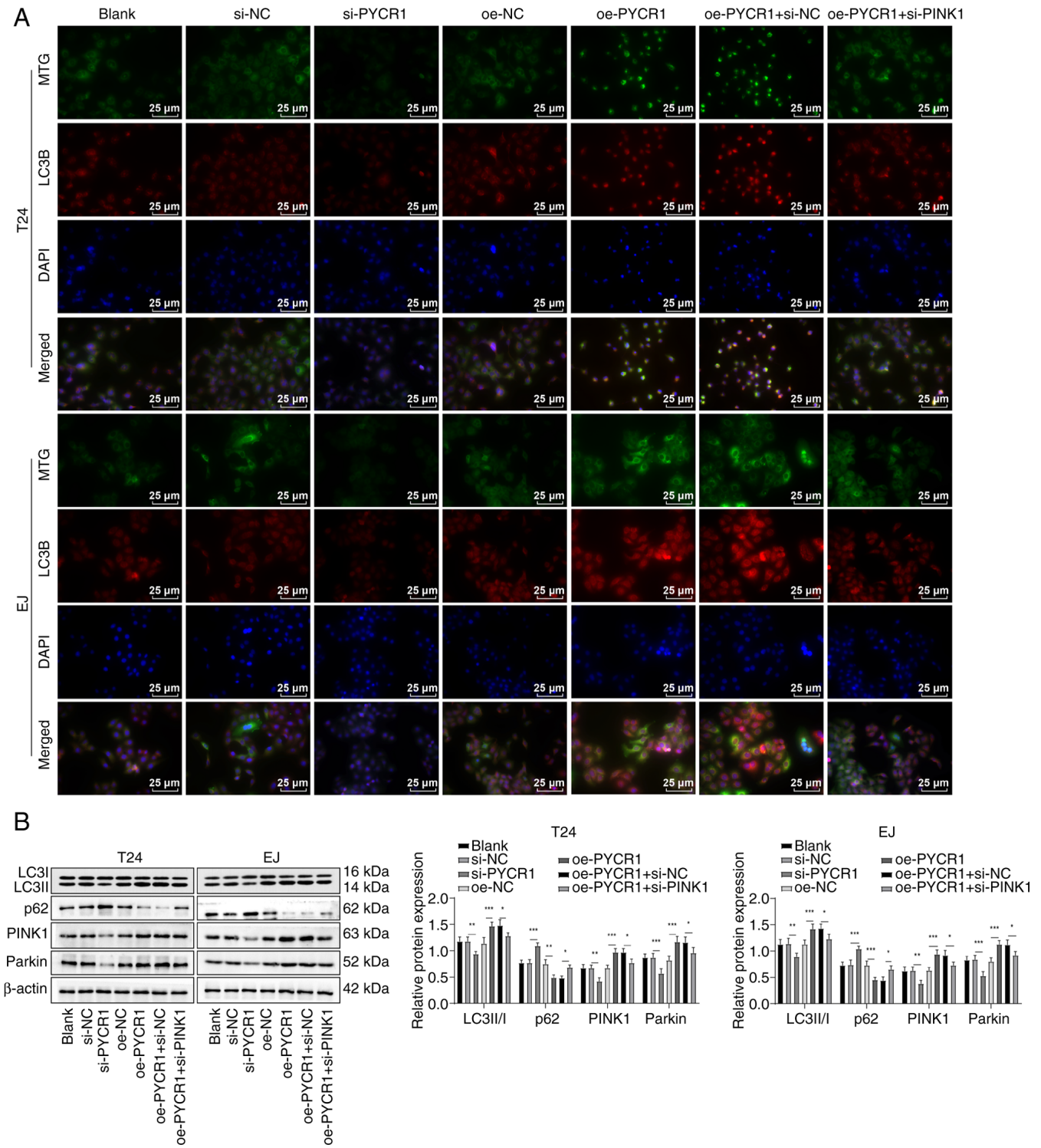

Figure 5. Continued.

those in the BC + Lv-oe-SMYD2 + si-NC group (Fig. 6A-C). HE staining showed that compared with the BC + Lv-oe-NC group, the tumor cell density of the BC + Lv-oe-SMYD2 group was elevated and the proportion of necrotic cells (unstructured eosinophilic substances) were decreased; compared with the BC + Lv-oe-SMYD2 + si-NC group, the tumor cell density of nude mice in the BC + Lv-oe-SMYD2 + Lv-si-PYCR1 group was decreased and the proportion of necrotic cells increased (Fig. 6D). By contrast with the BC + Lv-oe-NC group, protein levels of SMYD2, PYCR1, PINK1 and Parkin in tissue homogenate of nude mice in the BC + Lv-oe-SMYD2 group were elevated (Fig. 6E). SMYD2, Parkin, PYCR1 and PINK1 expression in the BC + Lv-oe-SMYD2 + Lv-si-PYCR1 group was lower than in the BC + Lv-oe-SMYD2 + si-NC group (Fig. 6E). As demonstrated by IHC results, SMYD2-, H3K4me3-, CD44- and CD133-positive cell numbers in the BC + Lv-oe-SMYD2 group were significantly augmented relative to the BC + Lv-oe-NC group; nude

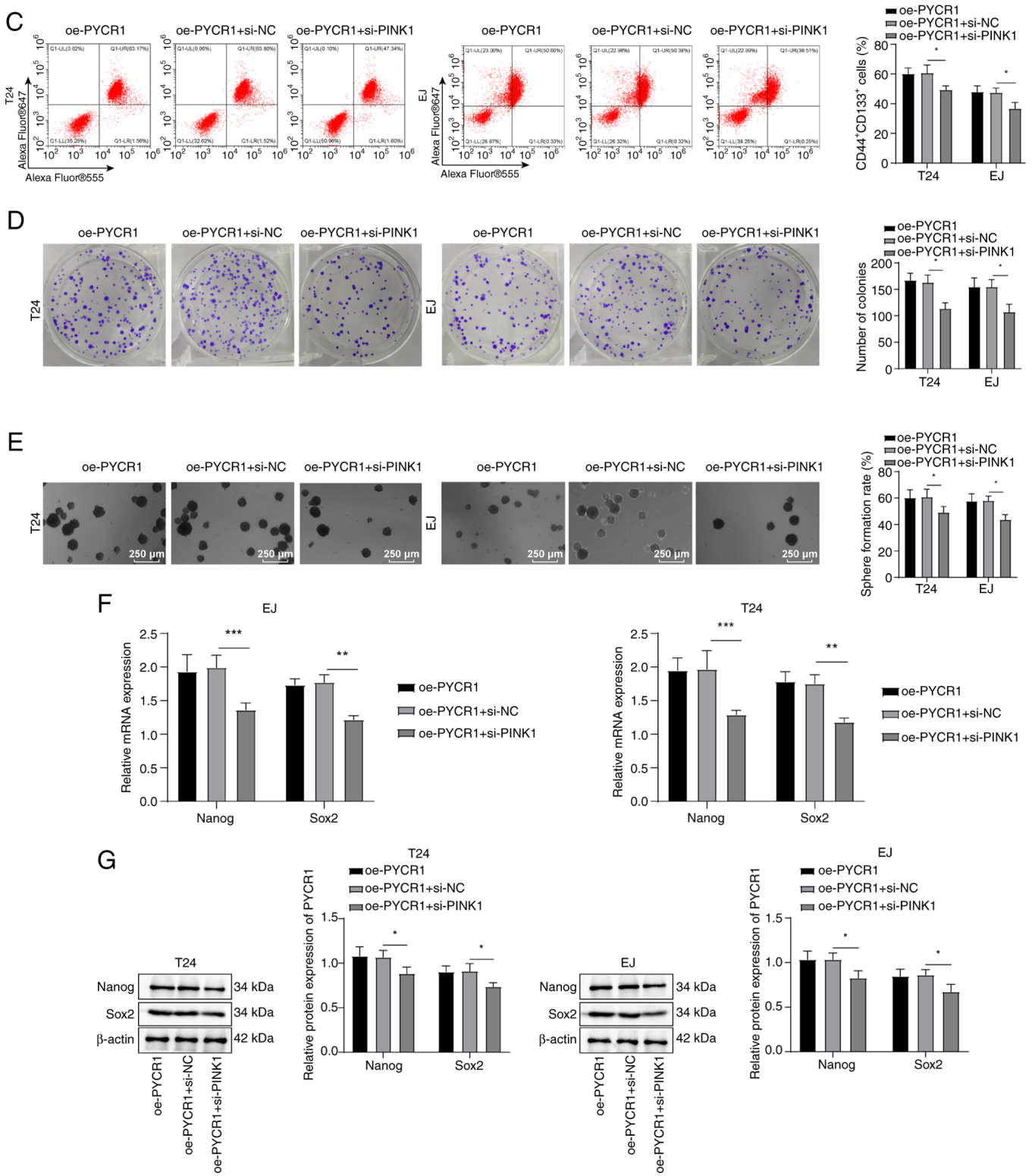

Figure 5. PYCR1 promotes bladder CSC stemness sustenance via the PINK1/Parkin pathway. (A) Immunofluorescence detection of mitochondrial (MTG; green) and autophagy marker (LC3B; red) expression. (B) Assessment of the protein levels of LC3B II/I, p62, PINK1 and Parkin by western blot. (C) Measurement of $CD44^+CD133^+$ cell level by flow cytometry. (D) Colony formation assay. (E) CSC sphere-forming assay to estimate tumor stemness. Expression of stemness marker proteins Nanog and Sox2 (F) mRNA and (G) protein was assessed by reverse transcription-quantitative PCR and western blot. *P<0.05, **P<0.01, ***P<0.001. SMYD2, SET and MYND domain-containing protein 2; PYRC1, pyrroline-5-carboxylate reductase 1; si, small-interfering; NC, negative control; oe, overexpression; PINK1, PTEN-induced putative kinase 1; MTG, Mito-Tracker Green; CSC, cancer stem cell.

mice in the BC + Lv-oe-SMYD2 + Lv-si-PYCR1 group displayed lower CD133- and CD44-positive cell numbers than those in the BC + Lv-oe-SMYD2 + si-NC group (Fig. 6F). Western blot results revealed that nude mice in the BC + Lv-oe-SMYD2 group exhibited a higher LC3B II/I ratio and lower p62 protein levels than the BC + Lv-oe-NC group;

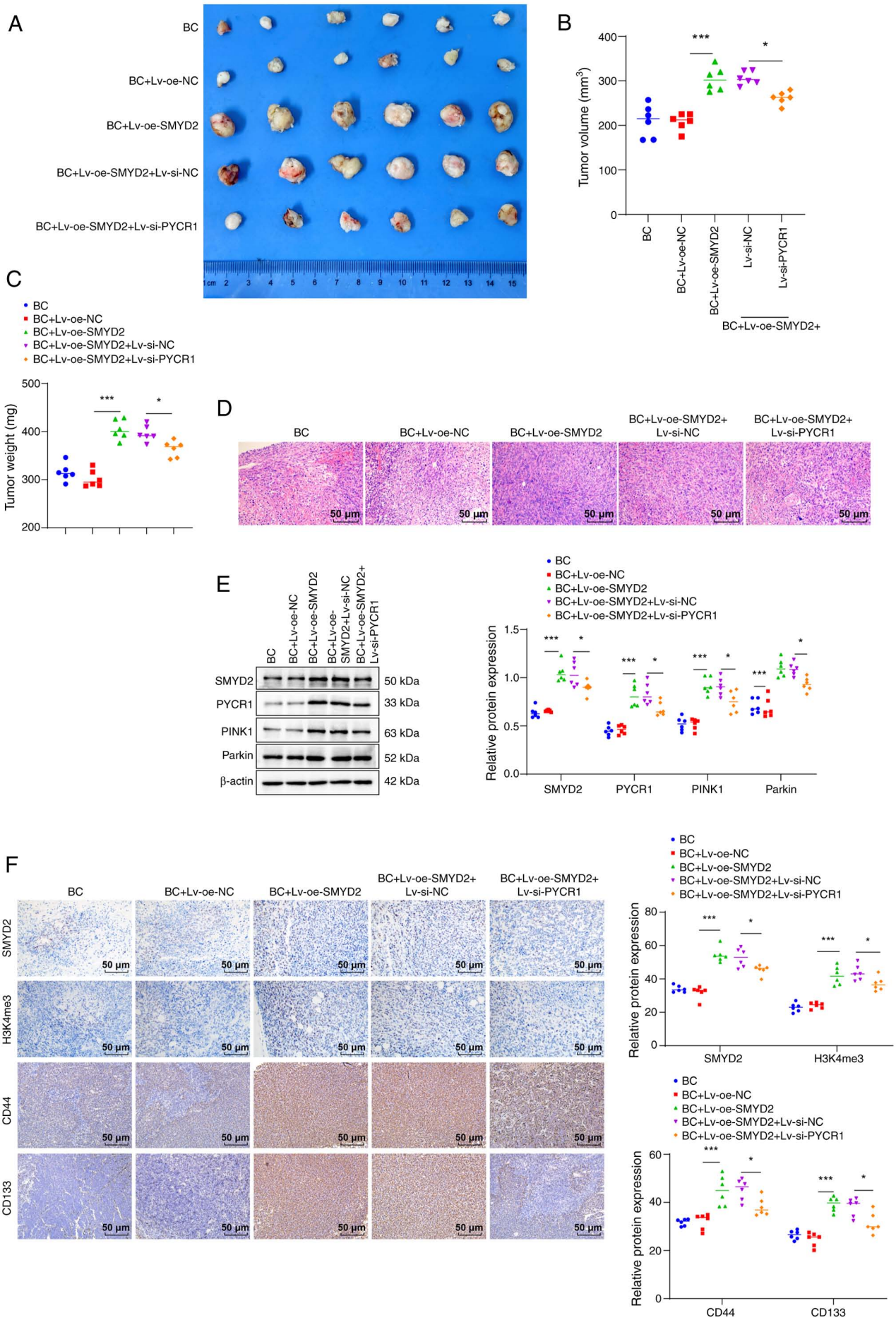

Figure 6. Continued.

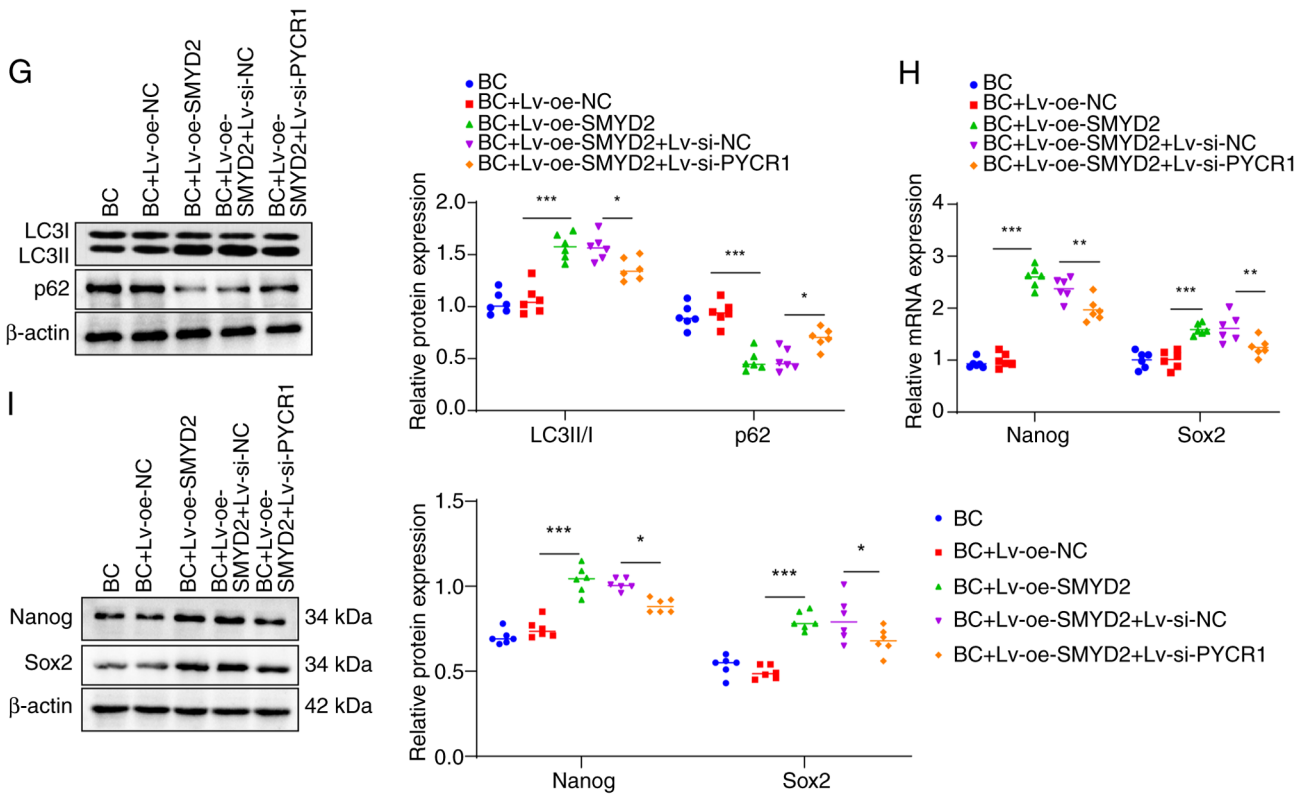

Figure 6. SMYD2 increases the maintenance of bladder cancer stem cell stemness by upregulating PYCR1 to stimulate the PINK1/Parkin pathway. Tumor (A) size, (B) volume and (C) weight. (D) Hematoxylin-eosin staining to detect pathological changes in tumor tissue. (E) Western blot to measure SMYD2, PYCR1, PINK1 and Parkin levels in nude mouse tissue homogenate. (F) Immunohistochemistry was performed to detect the number of SMYD2-, H3K4me3-, CD44- and CD133-positive cells in tumor tissues. (G) Protein expression of autophagy markers LC3B II/I and p62 was determined by western blotting. (H) Expression of stemness marker proteins Nanog and Sox2 mRNA was measured by reverse transcription-quantitative PCR. (I) Western blot assay to detect protein levels of Nanog and Sox2 in tissue homogenates of nude mice. *P<0.05, **P<0.01, ***P<0.001. SMYD2, SET and MYND domain-containing protein 2; PYCR1, pyrroline-5-carboxylate reductase 1; PINK1, PTEN-induced putative kinase 1; H3K4me3, histone H3 lysine 4 trimethylation; BC, bladder cancer; Lv, lentiviral; oe, overexpression; NC, negative control; si, small-interfering.

BC + Lv-oe-SMYD2 + Lv-si-PYCR1 group exhibited a higher LC3B II/I ratio and lower p62 protein expression compared with BC + Lv-oe-SMYD2 + si-NC group (Fig. 6G). Moreover, Nanog and Sox2 protein levels were raised in the BC + Lv-oe-SMYD2 group vs. BC + Lv-oe-NC group but these protein levels dropped in the BC + Lv-oe-SMYD2 + Lv-si-PYCR1 compared with BC + Lv-oe-SMYD2 + si-NC group (Fig. 6H and I). In summary, these results indicated that SMYD2 sustained BCSC stemness by increasing PYCR1 expression to stimulate the PINK1/Parkin mitophagy pathway.

Discussion

Lysine methyltransferases, which affect numerous oncoproteins and tumor suppressor proteins, play a key role in the development of various types of malignancies, such as colorectal cancer and lung cancer (25-27). SMYD2, an extensively studied lysine methyltransferase, is associated with regulation of transcription, epigenetics and tumorigenesis (28,29). However, the potential impact of SMYD2 on the stemness maintenance of BCSCs remains unclear. The present study demonstrated that histone methyltransferase SMYD2 is involved in the stemness of BCSCs by upregulating PYCR1 expression and activating the PINK1/Parkin pathway (Fig. 7).

PYCR1 strengthens BC proliferation and EMT, which is associated with expression of stemness markers Nanog and Sox2 (4,30), suggesting that PYCR1 plays a role in BCSC stemness. GEPIA database analysis demonstrated that SMYD2 was significantly highly expressed in BC. Correspondingly, SMYD2 expression is significantly increased in human BC compared with normal bladder tissue, underscoring that inhibiting SMYD2 may have therapeutic promise for BC (31). The present study assessed the mechanism of SMYD2/PYCR1 in maintaining BCSC stemness. CD44, a hallmark of BCSCs, indicates stemness and activates many signaling pathways to maintain self-renewal capacity (32,33). The potential role of CD44 and CD133 as markers for BCSCs has been proposed (34). PYCR1 and SMYD2 knockdown in $CD44^{+}CD133^{+}$ BCSC subpopulation with stem cell-like characteristics decreased $CD44^{+}CD133^{+}$ cell levels, Nanog and Sox2 expression and colony and sphere formation, whereas overexpressing PYCR1 or SMYD2 resulted the opposite effects. Similarly, suppression of PYCR1 *in vitro* decreases colony formation and proliferation and induces cell cycle arrest (35). Cui *et al* (20) confirmed that ablation of PYCR1 can lead to reduced expression of Sox2 and Nanog, CSC-associated aldehyde dehydrogenase^{+} population and ability of breast CSCs to form spheres, suggesting that PYCR1 is involved in preserving the stemness of breast cancer cells. In addition, Shang and Wei (36) demonstrated

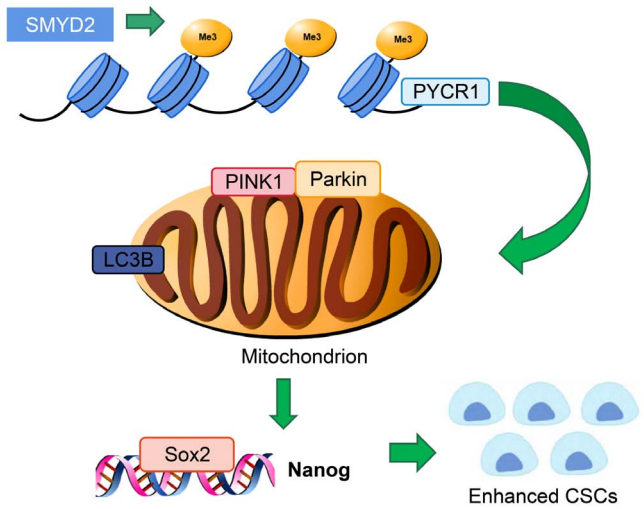

Figure 7. SMYD2 upregulates PYCR1 expression via H3K4me3, thereby activating the PINK1/Parkin mitophagy pathway, promoting expression of stem cell marker proteins Sox2 and Nanog and maintaining the stemness of bladder CSCs. SMYD2, SET and MYND domain-containing protein 2; PYCR1, pyrroline-5-carboxylate reductase 1; H3K4me3, histone H3 lysine 4 trimethylation; PINK1, PTEN-induced putative kinase 1; CSC, cancer stem cell; LC3B, light chain-3B; Sox2, SRY-box transcription factor 2.

that inhibition of SMYD2 impedes tumor sphere formation and cell migration in non-small-cell lung cancer cells. To the best of our knowledge, the impact of SMYD2 on the stemness of BCSCs has not been reported. It was hypothesized that both SMYD2 and PYCR1 amplified maintenance of stemness in BCSCs.

H3K4me3 is abnormally expressed in lung, liver and colon cancer (37-39). SMYD2 serves as a histone methyltransferase of H3K4me3, facilitating transcriptional activation of its downstream target genes by catalyzing trimethylation of histone H3K4, which is associated with modulation of target gene transcription (12,40). A notable positive association between SMYD2 and PYRC1 was observed in the present study. To the best of our knowledge, the present study is the first to demonstrate that SMYD2 may promote PYCR1 expression via H3K4me3; *in vitro* demonstrated increased PYCR1 and H3K4me3 levels, along with heightened enrichment levels of H3K4me3 in the PYCR1 promoter region in SMYD2-overexpressing BC cells. Furthermore, previous research has confirmed that proline produced by PYCR1 can activate the cGMP/cGMP-dependent protein kinase signaling pathway, thereby enhancing breast cancer stemness (20). Here, SMYD2 heightened stemness in BCSCs by regulating PYCR1.

The PINK1/Parkin signaling pathway is one of the primary regulatory mechanisms of mitophagy (17). The accumulation of PINK1 augments PINK1/Parkin-mediated mitophagy, which efficiently removes impaired mitochondria (41). The feedforward signaling pathway, including PINK1 and Parkin, is responsible for facilitating mitophagy (42). Here, PYCR1 silencing resulted in elevated p62 and Parkin/PINK1 expression, as well as lessened LC3B expression and LC3B II/I ratios, which were negated by PYCR1 overexpression. This indicated that PYCR1 could mediate the Parkin/PINK1 mitophagy axis. Moreover, it is well-established that mitophagy encourages the obtainment of tumor cell stemness (14,43). The present experiments verified the promoting effect of the PINK1/Parkin mitophagy pathway in BCSC stemness. Other investigations have established a connection between mitophagy and SC stemness (44,45). Augmentation of mitophagy can contribute to the stemness of mesenchymal SCs (46). Conversely, the reduction of mitophagy-related PINK1/Parkin leads to diminished stemness of bone marrow-derived mesenchymal SCs, as indicated by decreased expression of stemness markers Sox2 and Octamer-binding transcription factor 4 (44). Here, PYCR1 stimulated stemness maintenance in BCSCs via the PINK1/Parkin mitophagy pathway. Furthermore, *in vivo* verification demonstrated that SMYD2 preserved BCSC stemness by activating the PINK1/Parkin mitophagy pathway via enhancement of PYCR1 expression.

In conclusion, the present study demonstrated the regulatory effect and mechanism by which SMYD2 affects PYCR1. Additionally, *in vitro* and *in vivo* experiments demonstrated the role of PYCR1 in modulating the PINK1/Parkin signaling pathway, which affects mitophagy and regulates stemness of BCSCs. However, the present study only verified that PYCR1 regulates mitophagy via regulation of PINK1/Parkin to regulate BCSC stemness; other target genes and signaling pathways regulated by PYCR1 require further investigation. Upstream influencing factors of PYCR1 also need to be further explored. Future investigations investigate the role of mitophagy in preserving the stemness of CSCs, as well as the mechanisms by which PYCR1 modulates other target genes and signaling pathways.

Acknowledgements

Not applicable.

Funding

The present study was supported by Natural Science Foundation of Hunan Province (grant no. 2025JJ50640), Hunan Provincial Health High-Level Talent Scientific Research Project (grant no. R2023154) and Hunan Provincial People's Hospital Doctoral Fund Project (grant no. BSJJ202106).

Availability of data and materials

The data generated in the present study may be requested from the corresponding author.

Authors' contributions

All authors have read and approved the final manuscript. JC contributed to the study concepts, study design; SX and XY performed the literature review. JC and YW performed experiments. JC and WS contributed to the data analysis. JC and SX wrote and revised the manuscript. JC and SX confirm the authenticity of all the raw data.

Ethics approval and consent to participate

The present study was reviewed and approved by the Animal Ethics Committee of Hunan Provincial People's Hospital,

The First Affiliated Hospital of Hunan Normal University (approval no. 2024-84).

Patient consent for publication

Not applicable.

Competing interests

The authors declare that they have no competing interests.

References

1. Chen S, Zhu J, Wang F, Guan Z, Ge Y, Yang X and Cai J: LncRNAs and their role in cancer stem cells. Oncotarget 8: 110685-110692, 2017.
2. Eid RA, Alaa Edeen M, Shedid EM, Kamal AS, Warda MM, Mamdouh F, Khedr SA, Soltan MA, Jeon HW, Zaki MS and Kim B: Targeting Cancer Stem Cells as the Key Driver of Carcinogenesis and Therapeutic Resistance. Int J Mol Sci 24, 2023.
3. Aghaalikhani N, Rashtchizadeh N, Shadpour P, Allameh A and Mahmoodi M: Cancer stem cells as a therapeutic target in bladder cancer. J Cell Physiol 234: 3197-3206, 2019.
4. Li Z, Liu J, Fu H, Li Y, Liu Q, Song W and Zeng M: SENP3 affects the expression of PYCR1 to promote bladder cancer proliferation and EMT transformation by deSUMOylation of STAT3. Aging (Albany NY) 14: 8032-8045, 2022.
5. Song W, Li Z, Yang K, Gao Z, Zhou Q and Li P: Antisense lncRNA-RP11-498C9.13 promotes bladder cancer progression by enhancing reactive oxygen species-induced mitophagy. J Gene Med 25: e3527, 2023.
6. Song W, Yang K, Luo J, Gao Z and Gao Y: Dysregulation of USP18/FTO/PYCR1 signaling network promotes bladder cancer development and progression. Aging (Albany NY) 13: 3909-3925, 2021.
7. Zhang Y, Zhang X, Huang X, Tang X, Zhang M, Li Z, Hu X, Zhang M, Wang X and Yan Y: Tumor stemness score to estimate epithelial-to-mesenchymal transition (EMT) and cancer stem cells (CSCs) characterization and to predict the prognosis and immunotherapy response in bladder urothelial carcinoma. Stem Cell Res Ther 14: 15, 2023.
8. Ye Y, Li L, Dai Q, Liu Y and Shen L: Comprehensive analysis of histone methylation modification regulators for predicting prognosis and drug sensitivity in lung adenocarcinoma. Front Cell Dev Biol 10: 991980, 2022.
9. McCabe MT, Mohammad HP, Barbash O and Kruger RG: Targeting Histone Methylation in Cancer. Cancer J 23: 292-301, 2017.
10. Tan Z, Fu S, Feng R, Huang Y, Li N, Wang H and Wang J: Identification of potential biomarkers for progression and prognosis of bladder cancer by comprehensive bioinformatics analysis. J Oncol 2022: 1802706, 2022.
11. Xu W, Chen F, Fei X, Yang X and Lu X: Overexpression of SET and MYND domain-containing protein 2 (SMYD2) is associated with tumor progression and poor prognosis in patients with papillary thyroid carcinoma. Med Sci Monit 24: 7357-7365, 2018.
12. Xu H, Ba Z, Liu C and Yu X: Long noncoding RNA DLEU1 promotes proliferation and glycolysis of gastric cancer cells via APOC1 upregulation by recruiting SMYD2 to induce trimethylation of H3K4 modification. Transl Oncol 36: 101731, 2023.
13. Whelan KA, Chandramouleeswaran PM, Tanaka K, Natsuizaka M, Guha M, Srinivasan S, Darling DS, Kita Y, Natsugoe S, Winkler JD, *et al*: Autophagy supports generation of cells with high CD44 expression via modulation of oxidative stress and Parkin-mediated mitochondrial clearance. Oncogene 36: 4843-4858, 2017.
14. Liu K, Lee J, Kim JY, Wang L, Tian Y, Chan ST, Cho C, Machida K, Chen D and Ou JJ: Mitophagy controls the activities of tumor suppressor p53 to regulate hepatic cancer stem cells. Mol Cell 68: 281-292, 2017.
15. Panigrahi DP, Praharaj PP, Bhol CS, Mahapatra KK, Patra S, Behera BP, Mishra SR and Bhutia SK: The emerging, multifaceted role of mitophagy in cancer and cancer therapeutics. Semin Cancer Biol 66: 45-58, 2020.
16. Lou Y, Ma C, Liu Z, Shi J, Zheng G, Zhang C and Zhang Z: Antimony exposure promotes bladder tumor cell growth by inhibiting PINK1-Parkin-mediated mitophagy. Ecotoxicol Environ Saf 221: 112420, 2021.
17. Nguyen TN, Padman BS and Lazarou M: Deciphering the molecular signals of PINK1/Parkin mitophagy. Trends Cell Biol 26: 733-744, 2016.
18. Lee J, Liu K, Stiles B and Ou JJ: Mitophagy and hepatic cancer stem cells. Autophagy 14: 715-716, 2018.
19. Choudhury D, Rong N, Senthil Kumar HV, Swedick S, Samuel RZ, Mehrotra P, Toftegaard J, Rajabian N, Thiyagarajan R, Podder AK, *et al*: Proline restores mitochondrial function and reverses aging hallmarks in senescent cells. Cell Rep 43: 113738, 2024.
20. Cui B, He B, Huang Y, Wang C, Luo H, Lu J, Su K, Zhang X, Luo Y, Zhao Z, *et al*: Pyrroline-5-carboxylate reductase 1 reprograms proline metabolism to drive breast cancer stemness under psychological stress. Cell Death Dis 14: 682, 2023.
21. Zietzer A, Hosen MR, Wang H, Goody PR, Sylvester M, Latz E, Nickenig G, Werner N and Jansen F: The RNA-binding protein hnRNPU regulates the sorting of microRNA-30c-5p into large extracellular vesicles. J Extracell Vesicles 9: 1786967, 2020.
22. Livak KJ and Schmittgen TD: Analysis of relative gene expression data using real-time quantitative PCR and the 2(-Delta Delta C(T)) Method. Methods 25: 402-408, 2001.
23. Han Y, Liu C, Zhang D, Men H, Huo L, Geng Q, Wang S, Gao Y, Zhang W, Zhang Y and Jia Z: Mechanosensitive ion channel Piezo1 promotes prostate cancer development through the activation of the Akt/mTOR pathway and acceleration of cell cycle. Int J Oncol 55: 629-644, 2019.
24. Dai X, Ren T, Zhang Y and Nan N: Methylation multiplicity and its clinical values in cancer. Expert Rev Mol Med 23: e2, 2021.
25. Komatsu S, Ichikawa D, Hirajima S, Nagata H, Nishimura Y, Kawaguchi T, Miyamae M, Okajima W, Ohashi T, Konishi H, *et al*: Overexpression of SMYD2 contributes to malignant outcome in gastric cancer. Br J Cancer 112: 357-364, 2015.
26. Zhang Y, Zhou L, Xu Y, Zhou J, Jiang T, Wang J, Li C, Sun X, Song H and Song J: Targeting SMYD2 inhibits angiogenesis and increases the efficiency of apatinib by suppressing EGFL7 in colorectal cancer. Angiogenesis 26: 1-18, 2023.
27. Kim K, Ryu TY, Jung E, Han TS, Lee J, Kim SK, Roh YN, Lee MS, Jung CR, Lim, JH, *et al*: Epigenetic regulation of SMAD3 by histone methyltransferase SMYD2 promotes lung cancer metastasis. Exp Mol Med 55: 952-964, 2023.
28. Sakamoto LH, Andrade RV, Felipe MS, Motoyama AB and Pittella Silva F: SMYD2 is highly expressed in pediatric acute lymphoblastic leukemia and constitutes a bad prognostic factor. Leuk Res 38: 496-502, 2014.
29. Yi X, Jiang XJ and Fang ZM: Histone methyltransferase SMYD2: Ubiquitous regulator of disease. Clin Epigenetics 11: 112, 2019.
30. Migita T, Ueda A, Ohishi T, Hatano M, Seimiya H, Horiguchi SI, Koga F and Shibasaki F: Epithelial-mesenchymal transition promotes SOX2 and NANOG expression in bladder cancer. Lab Invest 97: 567-576, 2017.
31. Cho HS, Hayami S, Toyokawa G, Maejima K, Yamane Y, Suzuki T, Dohmae N, Kogure M and Kang D: RB1 methylation by SMYD2 enhances cell cycle progression through an increase of RB1 phosphorylation. Neoplasia 14: 476-486, 2012.
32. Gao RL, Chen XR, Li YN, Yan XY, Sun JG, He QL and Cai FZ: Upregulation of miR-543-3p promotes growth and stem cell-like phenotype in bladder cancer by activating the Wnt/β-catenin signaling pathway. Int J Clin Exp Pathol 10: 9418-9426, 2017.
33. Hu Y, Zhang Y, Gao J, Lian X and Wang Y: The clinicopathological and prognostic value of CD44 expression in bladder cancer: A study based on meta-analysis and TCGA data. Bioengineered 11: 572-581, 2020.
34. Xia P, Liu DH, Xu ZJ and Ren F: Cancer stem cell markers for urinary carcinoma. Stem Cells Int 2022: 3611677, 2022.
35. Cai F, Miao Y, Liu C, Wu T, Shen S, Su X and Shi Y: Pyrroline-5-carboxylate reductase 1 promotes proliferation and inhibits apoptosis in non-small cell lung cancer. Oncol Lett 15: 731-740, 2018.
36. Shang L and Wei M: Inhibition of SMYD2 sensitized cisplatin to resistant cells in NSCLC through activating p53 pathway. Front Oncol 9: 306, 2019.

37. Lin X, Chen JD, Wang CY, Cai Z, Zhan R, Yang C, Zhang LY, Li LY, Xiao Y, Chen MK and Wu M: Cooperation of MLL1 and Jun in controlling H3K4me3 on enhancers in colorectal cancer. Genome Biol 24: 268, 2023.
38. Phoyen S, Sanpavat A, Ma-On C, Stein U, Hirankarn N, Tangkijvanich P, Jindatip D, Whongsiri P and Boonla C: H4K20me3 upregulated by reactive oxygen species is associated with tumor progression and poor prognosis in patients with hepatocellular carcinoma. Heliyon 9: e22589, 2023.
39. Zhou Z, Zhang B, Deng Y, Deng S, Li J, Wei W, Wang Y, Wang J, Feng Z, Che M, *et al*: FBW7/GSK3 β mediated degradation of IGF2BP2 inhibits IGF2BP2-SLC7A5 positive feedback loop and radioresistance in lung cancer. J Exp Clin Cancer Res 43: 34, 2024.
40. Abu-Farha M, Lambert JP, Al-Madhoun AS, Elisma F, Skerjanc IS and Figeys D: The tale of two domains: proteomics and genomics analysis of SMYD2, a new histone methyltransferase. Mol Cell Proteomics 7: 560-572, 2008.
41. Wang S, Long H, Hou L, Feng B, Ma Z, Wu Y, Zeng Y, Cai J, Zhang DW and Zhao G: The mitophagy pathway and its implications in human diseases. Signal Transduct Target Ther 8: 304, 2023.
42. Silvian LF: PINK1/parkin pathway activation for mitochondrial quality control-which is the best molecular target for therapy? Front Aging Neurosci 14: 890823, 2022.
43. Yuan X, Chen K, Zheng F, Xu S, Li Y, Wang Y, Ni H, Wang F, Cui Z, Qin Y, *et al*: Low-dose BPA and its substitute BPS promote ovarian cancer cell stemness via a non-canonical PINK1/p53 mitophagic signaling. J Hazard Mater 452: 131288, 2023.
44. Feng X, Yin W, Wang J, Feng L and Kang YJ: Mitophagy promotes the stemness of bone marrow-derived mesenchymal stem cells. Exp Biol Med (Maywood) 246: 97-105, 2021.
45. Liu D, Sun Z, Ye T, Li J, Zeng B, Zhao Q, Wang J and Xing HR: The mitochondrial fission factor FIS1 promotes stemness of human lung cancer stem cells via mitophagy. FEBS Open Bio 11: 1997-2007, 2021
46. Vazquez-Martin A, Van den Haute C, Cufi S, Corominas-Faja B, Cuyàs E, Lopez-Bonet E, Rodriguez-Gallego E, Fernández-Arroyo S, Joven J, Baekelandt V and Menendez JA: Mitophagy-driven mitochondrial rejuvenation regulates stem cell fate. Aging (Albany NY) 8: 1330-1352, 2016.